Optica Applicata, Vol. LIV, No. 3, 2024
DOI: 10.37190/oa240310

Numerical study of LED-pumped Nd:KGW laser

Feruza SHERMATOVA*, Shermakhamat PAYZIYEV, Anvarjon SHERNIYOZOV

Institute of Ion-Plasma and Laser Technologies, 33 Durmon yuli, Tashkent 100125, Uzbekistan

*Corresponding author: feruzashermatova.iplt@gmail.com

In this study, we conducted a numerical analysis of LED-pumped solid-state lasers. We developed a simulation model for LED-pumped Nd:KGW and Nd:YAG lasers, incorporating a "five-way" pumping module. The spectral and laser characteristics of Nd:KGW were analyzed. Our results indicate that Nd:KGW crystals may be more suitable for LED pumping compared to the widely used Nd:YAG, as evidenced by their comparative performance. LED pumped Nd:KGW laser showed higher slope efficiency. We provide estimates for the laser output and absorption distribution. The study explores the influence of Nd concentration levels within Nd:KGW on laser outputs when employing LED pumping, while also addressing thermal considerations in Nd:KGW rods.

Keywords: LEDs, LED-pumped lasers, Nd:KGW, Nd:YAG.

1. Introduction

Light-emitting diodes (LEDs) are promising light sources. The first LED-pumped laser system was demonstrated in 1964 using a Dy:CaF_2 crystal [1]. In the 1970s, LEDs were used as pumping sources for several laser crystals [2-6]. However, the concept of LED pumping encountered stagnation, partly due to the advent of high-efficiency laser diodes with more appealing characteristics. Recently, the rapid development of LED lighting has renewed interest in LED pumping. Nowadays, LEDs are considered promising pumping sources due to their high electrical-to-optical efficiency, low cost, compact design, and long operating lifetimes. LEDs are less sensitive to electrostatic discharges and have a longer lifetime, making them competitive with laser diodes. However, despite improvements in LED performance since the 1970s, LED-pumped lasers are still in the early stages of development due to several issues such as low overall power-to-power efficiency, technical issues, complexities in pumping schemes, and fundamental issues related to the spectral properties of the gain materials.

To date, various LED-pumped laser media have been reported, including polymers [7], fibers [8], semiconductors [9], and several dielectric laser crystals [10-18], mainly with YAG matrix [12-14, 17-18]. However, many other solid-state media that could be suitable for LED pumping have not been investigated yet, such as different ion-doped matrices. Restrictions such as the requirement for active ions in matrices with an absorption band in the visible range of the spectrum, as well as difficulties related to spectral overlapping and accounting for optical parameters (emission cross-section, lifetime, concentration of active ions, absorption coefficient, *etc*.), may pose obstacles to the progress of LED-pumped solid-state lasers. In this vein, crystals doped with neodymium have the most optimal parameters in the near-infrared range of the spectrum.

The availability of many suitable matrices (YAG, YLF, YVO_4, *etc*.) for neodymium ions creates more opportunities for LED pumping. In the case of neodymium, its possibilities with other potential matrices for LED pumping have not yet been fully studied. One such prospective matrix for neodymium is KGW, due to its high emission cross-section compared with other widely used and studied LED-pumping Nd^{3+}-doped laser crystals such as Nd:YAG and Nd:YVO_4. According to [19], flashlamp-pumped Nd:KGW lasers are more than twice as efficient as the corresponding Nd:YAG lasers and can compete with them under diode-pumped conditions [20]. An experimental study on Nd:KGW lasers pumped by LEDs has also been reported [21]. This study, which came to our attention during the later stages of manuscript preparation, found that the energy conversion efficiency of Nd:KGW was higher than that of Nd:YAG due to increased spectral overlap between LEDs and Nd:KGW.

The aim of the present study is to evaluate the performance of LED-pumped Nd:KGW lasers in comparison to Nd:YAG lasers using numerical simulations. While our study overlaps with previous research on Nd:KGW, we investigated the Nd:KGW crystal for LED pumping under different and new schematic conditions. Therefore, it provides additional insights and contributes to the existing literature. In this comparative study, to ensure identical pumping conditions for Nd:KGW and Nd:YAG lasers, a "five-way module," similar to the one experimentally used in a recent study on LED-pumped lasers, where the active medium was an Nd:YAG crystal, was used as a reference [18].

2. Laser characteristics of Nd:KGW crystal

A neodymium-doped potassium gadolinium tungstate crystal (Nd:KGW) is a prospective active medium for solid-state laser systems in the infrared region due to its wider absorption bandwidth at 808 nm and higher stimulated emission cross-section. The laser emission in an Nd-doped host crystal occurs at the $^4F_{3/2}$–$^4I_{11/2}$ transition [22]. Nd:YAG and Nd:YLF laser systems are commercially available and have been introduced into various applications in science and technology due to their convenient thermal, physical, and spectroscopic properties. However, the absorption peak in Nd-doped YAG and YLF is narrow around 808 nm due to their internal crystal structures. Because of the mismatched sizes of the active Nd^{3+} ions replacing the Y^{3+} ions in YAG and YLF host crystals, the concentration of active ions cannot be enhanced in these matrices. The ionic radius of gadolinium (Gd) is slightly larger than that of yttrium (Y) [23]. This difference in ionic radii allows for a higher concentration of neodymium (Nd) ions

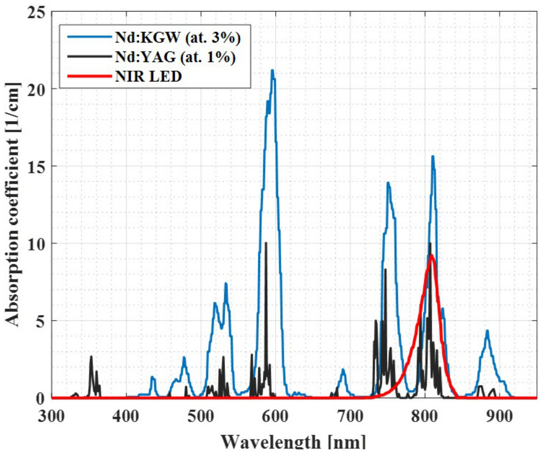

Fig. 1. Absorption spectra of Nd:KGW and Nd:YAG with emission spectrum of NIR LED.

in the Nd:KGW crystal, and the higher concentration of Nd ions ensures a significantly higher absorption peak (Fig. 1).

However, increasing the concentration of Nd ions shortens the fluorescence lifetime of the laser level, which can lead to a drop in the efficiency of the laser system [19]. While pump absorption increases linearly with Nd concentration, the radiative lifetime of the lasing transition decreases. Based on the data presented in Table 1, we can see that Nd:KGW could be a better alternative for developing compact and efficient LED-pumped lasers than Nd:YAG.

According to the conclusions of an experimental study [20], there are a few drawbacks associated with KGW as a host crystal for Nd ions. One drawback is that the thermal conductivity of KGW is much lower than that of YAG (12–14 W/mK). The thermal conductivity of KGW is 2.6–3.8 W/mK. This might lead to heat-load problems in

T a b l e 1. Laser parameters of Nd:YAG and Nd:KGW [20].

Parameters	Nd:YAG	Nd:KGW
Nd dopant concentration	1 at.%	3 at.%
Fluorescence lifetime	230 μs	130 μs
Stimulated emission cross-section	3.5×10^{-19} cm^2	3.7×10^{-19} cm^2
Emission wavelength	1064 nm	1067 nm
Refractive index	1.8	$n_p = 1.978$ $n_m = 2.014$ $n_g = 2.049$
Active ion concentration	1.38×10^{20} cm^{-3}	1.91×10^{20} cm^{-3}
Quantum yield	0.9–0.95	0.757 [24]
Thermal conductivity	12–14 W/mK	$K_a = 2.6$ W/mK $K_b = 3.8$ W/mK $K_c = 3.4$ W/mK

the lasing material [25], which can impact the overall efficiency of LED-pumped laser systems.

3. Simulation model

We used the Monte Carlo *photon* tracing method because of its flexibility and reliability in taking into account specific LED characteristics such as complex radiation patterns and spectral parameters, which require precise control. *Photon* tracing can be perceived as a modified ray tracing method that uses Monte Carlo techniques to control random processes. Our previous studies have demonstrated the versatility of photon tracing for modeling solar lasers [26-29]. For more details about Monte Carlo photon tracing, we suggest the following reference [30].

We developed a simulation model based on an experimental study in which a five -way pumping module was used to pump an Nd:YAG rod (5 mm in diameter, 110 mm in length). This construction, with a total of 80 LEDs, was designed with an intention of achieving uniform pumping and obtain a high-quality beam. The crystal was installed in the middle of a glass tube (with a refractive index of 1.5), and water (with a refractive index of 1.33) was used to cool the laser crystal (Fig. 2). Additionally, a reflectance with a coefficient of 0.9 for the cavity walls was introduced into the model. In Fig. 2(b), to ensure consistency with the laws of reflection and refraction at the boundary of two media, the normal for each photon passage is indicated.

It should be noted that according to the established algorithm, each photon emitted by the LED has only one chance of absorption, and each photon can reach the laser medium only if it undergoes refraction at the air–glass and glass–water boundaries. In cases where a photon is reflected at these boundaries, it automatically leaves the tracing system, as the chance of absorption for such photons is too small. Likewise, there is no accounting for photons passing through the water–glass interface after interacting with (but not being absorbed by) the active medium.

In the present model, the initial coordinates (x, y, z) are generated uniformly across the emitting surface of the LED, taking into account its geometric dimensions. The direction cosine components $a_x = \sin\theta\cos\varphi$, $a_y = \sin\theta\sin\varphi$, $a_z = \cos\theta$ are initialized ac-

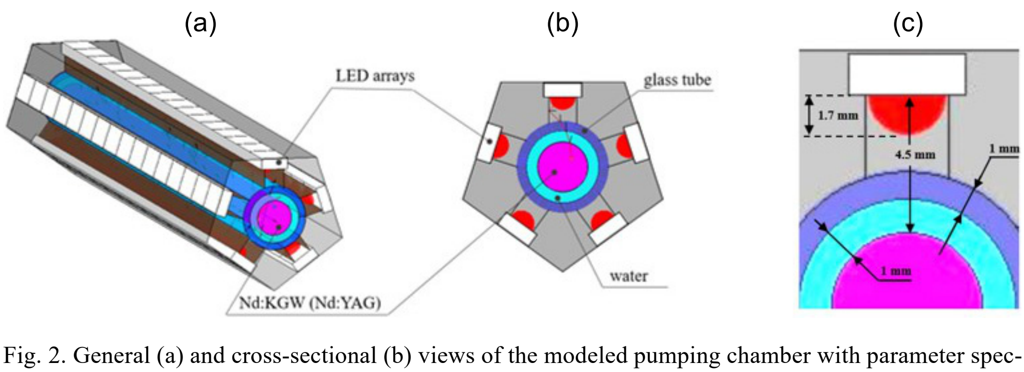

Fig. 2. General (a) and cross-sectional (b) views of the modeled pumping chamber with parameter specifications (c).

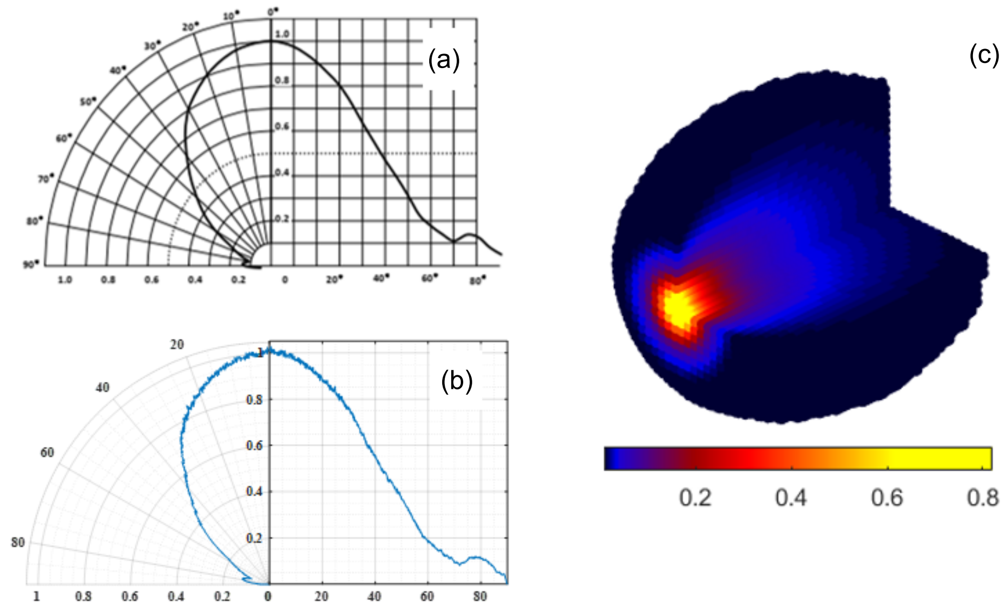

Fig. 3. Emission pattern of LUMINUS SST-10-IRD-B90H-S810: (a) from datasheet; (b) sampled θ with 10^6 photons statistics using Monte-Carlo technique; (c) 3D propagation model.

cording to the radiation pattern of the commercial LED (LUMINUS SST-10-IRD -B90H-S810). Specifically, the azimuthal angle is determined as $\varphi = 2\pi\xi$, where is a random variable uniformly distributed in the interval [0, 1]. The elevation angle is sampled from the radiation pattern provided in the datasheet (Fig. 3(a)). Figure 3(b) illustrates the emission spectrum generated via Monte Carlo simulation with a statistics of 10^6 photons.

The wavelength of emitted photons is sampled from the spectrum given in Fig. 1 and their respective absorption length. Absorption of a photon by the medium is one of the key features directly influencing the pumping process. It is known that not all propagated photons within the medium might be absorbed. The probability of photon annihilation (absorption) is linked to the absorption spectrum of the active medium. In the Monte Carlo photon tracing method, this process is governed by the inverse distribution and the Beer–Lambert law $l = -\ln\xi/\eta$, where l is the absorption length, ξ is a random number, and η is the absorption coefficient for the given wavelength. In this case, the absorption length, which is the distance the photon travels until it is absorbed, is limited by the length of the active medium. After the photon annihilation in the medium, the absorbed energy can contribute to raising the temperature of the medium or be sufficient to "creation" a new photon with a new wavelength from the emission spectrum of the active medium. The absorption point of the old photon is used as the coordinates for initiating the newly generated photon.

In the simulation model, we entered a distance of 4.5 mm between the laser rod surface and the LEDs luminescence center, a coolant tube outer diameter of 9 mm, and a thickness of 1 mm. (Fig. 2(c)). Regarding the choice of 4.5 mm, we explored distances ranging from 3.7 mm (where the LED lens touches the coolant tube) to 6 mm. As this distance increases, the efficiency of pumping and absorption decreases. The developed simulation model showed consistent and realistic behavior. The model can be valuable for comparing the output characteristics of laser systems based on Nd:KGW and Nd:YAG under identical pumping conditions. Full validation of the model is not provided here, primarily because the applicability of the Monte Carlo photon tracing method has been repeatedly demonstrated and validated through experimental studies [26-30]. Furthermore, the current work is considered a comparative study.

4. Results and discussions

The main goal of the developed simulation model was to evaluate the potential of Nd:KGW as an active medium for LED pumping compared to the widely used Nd:YAG medium. Based on initial data derived from the simulation model, we observed that the absorption efficiency of Nd:KGW significantly surpassed that of Nd:YAG. The absorption distributions and relative color bar shown in Fig. 4 illustrate the pumping efficiencies, uniformity, and heterogeneity of the absorbed power distribution. These factors play a crucial role in influencing laser beam quality. The distribution was computed with statistics from 10 million photons emitted by each LED, and the values in the color panel correspond to the number of absorbed photons in each

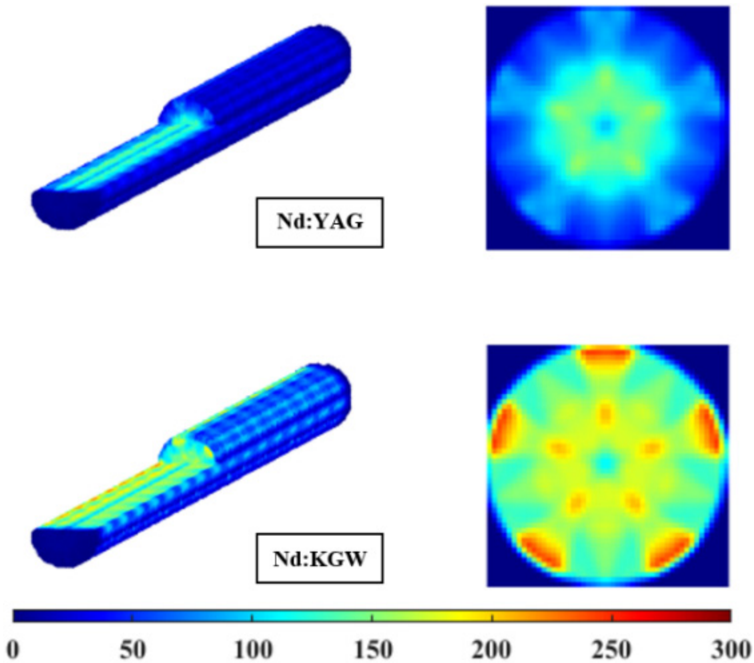

Fig. 4. Absorption distribution.

volumetric cell (the laser crystal is divided into $50 \times 50 \times 200$ cells along the x, y, and z axes). In subsequent evaluations of laser performance, this absorption distribution will be normalized.

This outcome was anticipated due to the higher concentration of active neodymium ions and the greater spectral overlap in the KGW matrix. The absorption efficiency estimated from simulations demonstrates the superiority of Nd:KGW (66.2%) over Nd:YAG (37.1%) in terms of absorbed photon percentage (3% and 1%, respectively).

We initially assessed the influence of Nd concentration levels within Nd:KGW on laser properties. This interest was triggered by previous studies [19, 32-34], which highlighted significant performance variations associated with different concentration levels. While studies on Nd:KGW crystals with concentrations ranging from 1% to 10% exist, comprehensive information regarding laser rods was absent, making it challenging to model all variations. Therefore, we focused on two specific Nd:KGW laser rods with doping concentrations of 3% and 5%. We incorporated the spectral and physical attributes of these Nd:KGW rods into the model, allowing us to calculate both pumping efficiencies and their corresponding distributions. Key parameters and model specifications are listed in Table 2 for comparative analysis.

Table 2. Laser parameters of Nd:KGW depending on concentration of active ions.

Nd dopant concentration	3 at.%	5 at.%
Active ion concentration	1.9×10^{20} cm^{-3} [20]	3.2×10^{20} cm^{-3} [35]
Fluorescence lifetime	130 μs [20]	120 μs [36]
Stimulated emission cross-section	3.7×10^{-19} cm^2 [20]	3.3×10^{-19} cm^2 [36]
Quantum yield	0.757 [24]	
Pumping efficiency	0.66 (estimated by the model)	0.71 (estimated by the model)

Since absorption distributions are not uniform, we had to use space dependent rate equations [28, 29]:

$$\varphi = \tau_c \iiint\limits_{\text{volume}} \frac{R_p(1+f) - f N_t/\tau}{(1+f) + V/(\varphi c \sigma_e \tau |u|^2)} \, dV \tag{1}$$

Here, the output power is then defined as $P_{out} = k\varphi$, where $k = h v \gamma_2 c / 2L_e$ is the proportionality coefficient (γ_2 is an output mirror transmission, L_e – the cavity length, h – Plank constant, v – laser frequency, c – speed of the light), which depends on resonator parameters (length of cavity = 150 mm, output coupler = 95%, internal losses = 0.002 cm^{-1}). In our calculations, we used the parameters of Nd^{3+} doped matrices listed in Table 1 and Table 2. The obtained results are plotted in Fig. 5.

The performance of the 5% Nd:KGW stands out as superior to the other two variants, albeit it closely resembles the performance of the 3% Nd:KGW. Henceforth, our focus in the remainder of this study is the comparative analysis between 3% Nd:KGW and 1% Nd:YAG (Fig. 6).

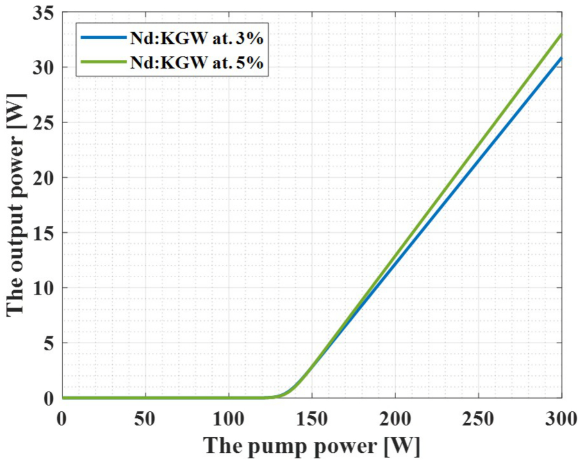

Fig. 5. Input–output power relationship.

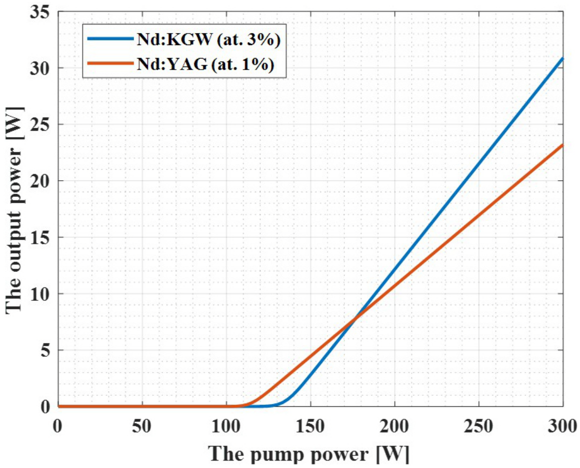

Fig. 6. Input–output power relationship (Nd:KGW *vs.* Nd:YAG).

Due to its superior absorption efficiency, Nd:KGW outperforms Nd:YAG, exhibiting higher slope efficiencies (17.9% and 12.1%, respectively). As anticipated from the properties of Nd:KGW, namely shorter fluorescence lifetime and lower quantum yield, it demonstrates a higher threshold power; however, this value remains relatively close to that of Nd:YAG. As an initial conclusion, the attainment of a high-power LED-pumped laser using Nd:KGW appears feasible.

4.1. Influence of thermal load on LED pumped Nd:KGW laser performance

Several studies [19-20, 37-39] highlight the suboptimal thermal properties of Nd:KGW for laser operations as a primary limitation. For instance, the study referenced in [20] reports that under pump powers reaching 6 W, laser rods with Nd doping concentrations of 4% and 8% experience fractures primarily due to differences in thermal expansion along orthogonal refractive index axes. As mentioned earlier, the results in Figs. 5 and 6, simulated under "optimal" cooling conditions, demonstrate the superior performance of Nd:KGW compared to Nd:YAG, especially within the achievable optical power range of up to 300 W, which is easily feasible with today's LED capabilities in the quasi-continuous wave (QCW) regime. According to LED specifications, LEDs can generate up to 2 W in continuous wave (CW) mode, totaling up to 160 W. Previous experimental studies [12, 18] on LED-pumped lasers have shown that LED power can be significantly scaled up in quasi-CW regimes. However, this raises an important question: Does the consideration of thermal loading significantly modify these outcomes? To explore this, our initial step involved computing the temperature distribution of the laser rods at varying pumping powers, while taking into account the corresponding physical properties of the rods. This computation is performed using the heat equation and parameters estimated by our model. Within the developed model, we have calculated the portion of pumping power that contributes to heating the medium using the following expression:

$$\eta_{\text{heat}} = \sum_i \left(\frac{hc}{\lambda^i_{\text{absorbed}}} - \frac{hc}{\lambda^i_{\text{laser}}} \right) / \sum_i \frac{hc}{\lambda^i_{\text{absorbed}}} \tag{2}$$

So, the estimated heat contributing coefficients are $\eta_{\text{heat}}^{\text{Nd:YAG}} = 0.1267$ and $\eta_{\text{heat}}^{\text{Nd:KGW}} = 0.3174$. These values are expected, primarily due to differences in spectral overlap between the pump and absorption spectra of the two rods. Concerning thermal conductivity, we chose the worst-case scenario, opting for the minimum value of 2.6 W/Km from the three options listed in Table 1. Additionally, we considered other crucial parameters: coolant flow rate (150 cm^3/s), heat transfer coefficient ($h = 0.75$ $\text{W/cm}^2\text{K}$), and the initial fluid temperature entering the cavity ($T_c = 20°\text{C}$). The temperature distributions calculated for Nd:YAG and Nd:KGW at varying pumping powers are illustrated in Fig. 7.

Nd:YAG exhibits minimal heating at both 300 and 600 W, maintaining a temperature difference between the crystal's center and edge below 5 degrees. In contrast, Nd:KGW displays a notable divergence, showing a temperature rise of 90 degrees at the higher power of 600 W, accompanied by a temperature gradient (difference between center and edge) of approximately 30 degrees. Employing a faster coolant flow rate could potentially alleviate this gradient, especially considering a side-pumping scheme similar to the one used in our model.

In this case, how can one interpret the earlier observed significant thermal issues with Nd:KGW [20] and the subsequent underperformance of Nd:KGW lasers? These negative thermal impacts on laser performance can be attributed to several factors: for laser diode-pumped configurations (end pumping), the temperature distribution becomes less uniform than depicted in Fig. 7, potentially leading to fractures. On the other hand,

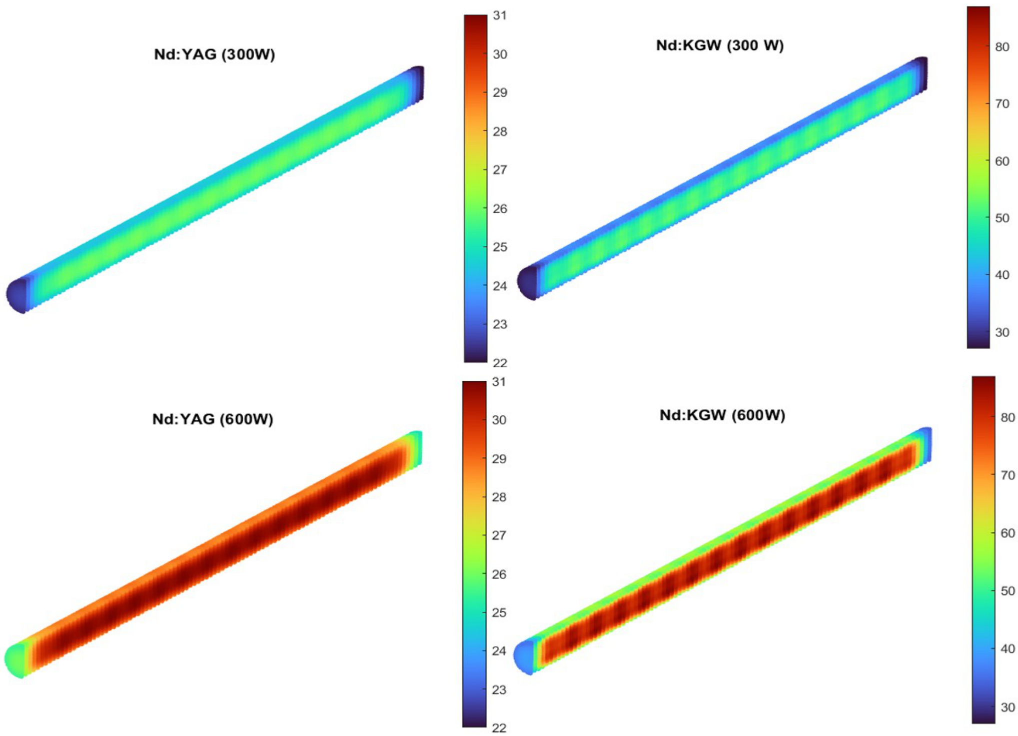

Fig. 7. Temperature distributions.

lamp-pumped sources exhibit significantly different spectral overlaps between the pump and absorption spectra compared to our present case. Hence, substantial heat problems are anticipated for lamp-based systems as well. However, we believe that the thermal challenges associated with Nd:KGW are not substantial when utilizing LED-pumped sources, as reasoned in our results. Additionally, the majority of LED-pumped lasers to date utilize pulsed pumping (quasi-CW), intended to increase optical power from LEDs, consequently further alleviating thermal concerns. Therefore, regarding the earlier question posed, thermal considerations should not alter the outcomes depicted in Fig. 6, which showcase the superior performance of Nd:KGW over traditional Nd:YAG.

Our findings generally agree with earlier published experimental results [21] on KGW lasers, suggesting that Nd:KGW can outperform Nd:YAG. However, there are some discrepancies. In our study using rods, the slope efficiencies were 17.9% and 12.1% for Nd:KGW and Nd:YAG lasers with direct LED pumping, respectively, compared to 18.3% and 5.5% reported in the aforementioned work with rectangular crystals.

5. Conclusions

In summary, our study focused on analyzing the lasing properties and performance of LED-pumped Nd:KGW lasers compared to Nd:YAG lasers using numerical simulations. To achieve this, we developed a simulation model for an LED-based laser featuring a five-way pumping module comprising a total of 80 LEDs. The developed model facilitated an in-depth analysis of the pumping process, providing estimations of various critical parameters such as absorption efficiencies and distributions essential for assessing laser performance.

We conducted a comparative analysis involving two Nd:KGW laser rods, specifically targeting doping concentrations of 3% and 5%, to determine the optimal doping level. Additionally, our investigation addressed thermal concerns associated with Nd:KGW, a significant issue observed in this crystal. Our findings suggest that Nd:KGW crystals might be more suitable for LED-based pumping compared to the widely utilized Nd:YAG. This potential could pave the way for high-power lasers utilizing LED-based pumping technologies.

Disclosures

The authors declare no conflicts of interest.

References

[1] Ochs S.A., Pankove J.I., *Injection-luminescence pumping of a $CaF_2:Dy^{2+}$ laser*, Proceedings of the IEEE **52**(6), 1964: 713-714. https://doi.org/10.1109/PROC.1964.3058

[2] Allen R.B., Scalise S.J., *Continuous operation of a YAIG: Nd laser by injection luminescent pumping*, Applied Physics Letters **14**(6), 1969: 188-190. https://doi.org/10.1063/1.1652768

[3] Reinberg A.R., Riseberg L.A., Brown R.M., Wacker R.W., Holton W.C., *GaAs: Si LED pumped Yb-doped YAG laser*, Applied Physics Letters **19**(1), 1971: 11-13. https://doi.org/10.1063/1.1653723

[4] Farmer G.I., Kiang Y.C., *Low-current-density LED-pumped Nd: YAG laser using a solid cylindrical reflector*, Journal of Applied Physics **45**(3), 1974: 1356-1371. https://doi.org/10.1063/1.1663413

[5] Saruwatari M., Kimura T., *LED pumped lithium neodymium tetraphosphate lasers*, IEEE Journal of Quantum Electronics **12**(10), 1976: 584-591. https://doi.org/10.1109/JQE.1976.1069047

[6] Ostermayer F., *LED end-pumped Nd: YAG lasers*, IEEE Journal of Quantum Electronics **13**(1), 1977: 1-6. https://doi.org/10.1109/JQE.1977.1069217

[7] Yang Y., Turnbull G.A., Samuel I.D.W., *Hybrid optoelectronics: A polymer laser pumped by a nitride light-emitting diode*, Applied Physics Letters **92**(16), 2008: 163306. https://doi.org/10.1063/1.2912433

[8] Htein L., Fan W., Han W.T., *Broad gain of the Er/Al-doped fiber amplifier by pumping with a white light-emitting diode*, Journal of Luminescence **146**, 2014: 87-90. https://doi.org/10.1016/j.jlumin.2013.09.066

[9] Liu X., Zhao G., Zhang Y., Deppe D.G., *Semiconductor laser monolithically pumped with a light emitting diode operating in the thermoelectrophotonic regime*, Applied Physics Letters **102**(8), 2013: 081116. https://doi.org/10.1063/1.4793656

[10] Lee K., Bae S., Kwak J.S., Kwon J.H., Yi J.H., *Study of a QCW light-emitting-diode (LED)-pumped solid-state laser*, Journal of the Korean Physical Society **59**(5), 2011: 3239-3245. https://doi.org/10.3938/jkps.59.3239

[11] Barbet A., Balembois F., Paul A., Blanchot J.-P., Viotti A.-L., Sabater J., Druon F., Georges P., *Revisiting of LED pumped bulk laser: First demonstration of Nd:YVO_4 LED pumped laser*, Optics Letters **39**(23), 2014: 6731-6734. https://doi.org/10.1364/OL.39.006731

[12] Villars B., Hill E.S., Durfee C.G., *Design and development of a high-power LED-pumped Ce:Nd:YAG laser*, Optics Letters **40**(13), 2015: 3049-3052. https://doi.org/10.1364/OL.40.003049

[13] Huang K.Y., Su C.K., Lin M.W., Chiu Y.C., Huang Y.C., *Efficient 750-nm LED-pumped Nd: YAG laser*, Optics Express **24**(11), 2016: 12043-12054. https://doi.org/10.1364/OE.24.012043

[14] CHO C.Y., PU C.C., SU K.W., CHEN Y.F., *LED-side-pumped Nd:YAG laser with >20% optical efficiency and the demonstration of an efficient passively Q-switched LED-pumped solid-state laser*, Optics Letters **42**(12), 2017: 2394-2397. https://doi.org/10.1364/OL.42.002394

[15] PICHON P., BARBET A., BLANCHOT J.P., DRUON F., BALEMBOIS F., GEORGES P., *Light-emitting diodes: A new paradigm for Ti:sapphire pumping*, Optica **5**(10), 2018: 1236-1239. https://doi.org/10.1364/OPTICA.5.001236

[16] PICHON P., DRUON F., BLANCHOT J.P., BALEMBOIS F., GEORGES P., *LED-pumped passively Q-switched Cr: LiSAF laser*, Optics Letters **43**(18), 2018: 4489-4492. https://doi.org/10.1364/OL.43.004489

[17] TARKASHVAND M., FARAHBOD A.H., HASHEMIZADEH S.A., *First demonstration of green and amber LED-pumped Nd: YAG laser*, Laser Physics **28**(5), 2018: 055801. https://doi.org/10.1088/1555-6611/aaa9ed

[18] SHEN J., JIANG S., HUANG X., JIANG R., LU P., XU S., *First demonstration of a LED-side-pumped acousto-optic Q-switched Nd: YAG rod laser with high repetition rate and beam quality operation*, Optical Materials **137**, 2023: 113596. https://doi.org/10.1016/j.optmat.2023.113596

[19] KUSHAWAHA V., MICHAEL A., MAJOR L., *Effect of Nd concentration on the Nd:KGW laser*, Applied Physics B **58**, 1994: 533-535. https://doi.org/10.1007/BF01081086

[20] GRAF T., BALMER J.E., *Lasing properties of diode laser-pumped Nd:KGW*, Advanced Solid State Lasers, OSA Proceedings Series, Optica Publishing Group, 1995, paper LM5.

[21] JUNG C., YI J., LEE B., LEE S., LIM J., JUNG W., KIM K., *Lasing characteristics of a LED-pumped Nd:KGW laser*, New Physics: Sae Mulli **68**(4), 2018: 477-485. https://doi.org/10.3938/NPSM.68.477

[22] KOECHNER W., *Solid-State Laser Engineering*, Vol. 1, Springer, 2013.

[23] LIDE D.R., *CRC Handbook of Chemistry and Physics*, 71st Ed., CRC Press, 1990, pp. 4-126.

[24] ABDOLVAND A.,WILCOX K.G., KALKANDJIEV T.K., RAFAILOV E.U., *Conical refraction Nd:KGd* $(WO_4)_2$ *laser*, Optics Express, **18**(3), 2010: 2753-2759. https://doi.org/10.1364/OE.18.002753

[25] TALUKDER R.C., EIBNA HALIM MD.Z., WARITANANT T., MAJOR A., *Multiwatt continuous wave Nd:KGW laser with hot-band diode pumping*, Optics Letters **41**(16), 2016: 3810-3812. https://doi.org/10.1364/OL.41.003810

[26] BAKHRAMOV S.A., SHERNIYOZOV A.A., PAYZIYEV S.D., ZIKRILLAYEV KH.F., KHALIKOV G.A., MAKHMUDOV KH.M., ISMAILOV M.Z., PAYZIEVA D.E., KHOTTCHENKOVA T.G., *Feasibility of luminophores in solar-pumped laser heads*, Journal of Applied Spectroscopy **88**(2), 2021: 370-372. https://doi.org/10.1007/s10812-021-01184-6

[27] SHERNIYOZOV A.A., PAYZIYEV S.D., *Solar pumped lasers: High-efficiency multi-pass side pumping scheme with Fresnel lens*, Applied Solar Energy **56**(6), 2020: 458-465. https://doi.org/10.3103/S0003701X20060092

[28] SHERNIYOZOV A.A., PAYZIYEV S.D., *Side-pumped efficient Ce:Nd:YAG solar laser in a multi-pass scheme*, Journal of Photonics for Energy **12**(3), 2022: 034501. https://doi.org/10.1117/1.JPE.12.034501

[29] PAYZIYEV S., SHERNIYOZOV A., *Influence of thermal population of lower laser levels on the performance of end-side-pumped Ce:Nd:YAG solar laser*, Journal of Photonics for Energy **12**(4), 2022: 044501. https://doi.org/10.1117/1.JPE.12.044501

[30] SHERNIYOZOV A., PAYZIYEV S., *Simulating optical processes: Monte Carlo photon tracing method*, Uzbek Journal of Physics **24**(3), 2022: 157-162.

[31] LED specifics provided by manufacturer: https://download.luminus.com/datasheets/Luminus_SST-10-IRD-BxxH_810_Datasheet.pdf

[32] ESMERIA J.M., ISHII H., SATO M., ITO H., *Efficient continuous-wave lasing operation of Nd:KGd* $(WO_4)_2$ *at 1.067 μm with diode and Ti:sapphire laser pumping*, Optics Letters **20**(14), 1995: 1538-1540. https://doi.org/10.1364/OL.20.001538

[33] KALISKY Y., KRAVCHIK L., LABBE C., *Repetitive modulation and passively Q-switching of diode -pumped Nd–KGW laser*, Optics Communications **189**(1-3), 2001: 113-125. https://doi.org/10.1016/S0030-4018(01)01018-5

[34] MUSSET O., BOQUILLON J.P., *Comparative laser study of Nd:KGW and Nd:YAG near 1.3 μm*, Applied Physics B **64**, 1997: 503-506. https://doi.org/10.1007/s003400050206

[35] BOULON G., METRAT G., MUHLSTEIN N., BRENIER A., KOKTA M.R., KRAVCHIK L., KALISKY Y., *Efficient diode-pumped Nd: KGd (WO4)2 laser grown by top nucleated floating crystal method*, Optical Materials **24**(1-2), 2003: 377-383. https://doi.org/10.1016/S0925-3467(03)00151-4

[36] KUSHAWAHA V., MICHAEL A., MAJOR L., *A comparative laser study of Nd: KGW and Nd: Cr: GSGG at 1.06 μm*, Spectroscopy Letters **29**(2), 1996: 293-297. https://doi.org/10.1080/00387019608001603

[37] YUMASHEV K.V., SAVITSKI V.G., KULESHOV N.V., PAVLYUK A.A., MOLOTKOV D.D., PROTASENYA A.L., *Laser performance of N_g-cut flash-lamp pumped Nd: KGW at high repetition rates*, Applied Physics B **89**, 2007: 39-43. https://doi.org/10.1007/s00340-007-2732-5

[38] SOULARD R., ZINOVIEV A., DOUALAN J.L., IVAKIN E., ANTIPOV O., MONCORGÉ R., *Detailed characterization of pump-induced refractive index changes observed in Nd:YVO_4, Nd:$GdVO_4$ and Nd:KGW*, Optics Express **18**(2), 2010: 1553-1568. https://doi.org/10.1364/OE.18.001553

[39] EIBNA HALIM M.Z., TALUKDER R.C., WARITANANT T., MAJOR A., *Passive mode locking of a Nd:KGW laser with hot-band diode pumping*, Laser Physics Letters, **13**(10), 2016: 105003. https://doi.org/10.1088/1612-2011/13/10/105003

Received April 8, 2024
in revised form June 20, 2024